electronics

Article

Enhancing NOMA's Spectrum Efficiency in a 5G Network through Cooperative Spectrum Sharing

Mohamed Hassan [1], Manwinder Singh [1,*], Khalid Hamid [2], Rashid Saeed [3], Maha Abdelhaq [4], Raed Alsaqour [5] and Nidhal Odeh [6]

1 Department of Wireless Communication, Lovely Professional University, Phagwara 144001, India
2 Department of Communication Systems Engineering, University of Science & Technology, Omdurman P.O. Box 30, Sudan
3 Department of Computer Engineering, College of Computers and Information Technology, Taif University, P.O. Box 11099, Taif 21944, Saudi Arabia
4 Department of Information Technology, College of Computer and Information Sciences, Princess Nourah Bint Abdulrahman University, P.O. Box 84428, Riyadh 11671, Saudi Arabia
5 Department of Information Technology, College of Computing and Informatics, Saudi Electronic University, P.O. Box 93499, Riyadh 11673, Saudi Arabia
6 School of Electrical, Computer and Telecommunications Engineering, Faculty of Engineering and Information Sciences, University of Wollongong, Wollongong 2500, Australia
* Correspondence: manwinder.2523@gmail.com or manwinder.25231@lpu.co.in

Abstract: Non-orthogonal multiple access (NOMA) is one of the most effective techniques for meeting the spectrum efficiency (SE) requirements of 5G and beyond networks. This paper presents two novel methods for improving the SE of the downlink (DL) NOMA power domain (PD) integrated with a cooperative cognitive radio network (CCRN) in a 5G network using single-input and single-output (SISO), multiple-input and multiple-output (MIMO), and massive MIMO (M-MIMO) in the same network and in a single cell. In the first method, NOMA users compete for free channels in a competing channel (C-CH) on the CCRN. The second method provides NOMA users with a dedicated channel (D-CH) with high priority. The proposed methods are evaluated using the Matlab software program using the three scenarios with different distances, power location coefficients, and transmitting power. Four users are assumed to operate on 80 MHz bandwidths (BWs) and use the quadrature phase shift keying (QPSK) modulation technique in all three scenarios. Successive interference cancellation (SIC) and unstable channel conditions are also considered when evaluating the performance of the proposed system under the assumption of frequency selective Rayleigh fading. The best four-user SE performance obtained by user $U4$ was 3.9 bps/Hz/cell for SISO DL NOMA, 5.1 bps/Hz/cell for SISO DL NOMA with CCRN with C-CH, and 7.2 bps/Hz/cell for SISO DL NOMA with CCRN with D-CH at 40 dBm transmit power. While 64 $\times$ 64 MIMO DL NOMA improved SE performance of the best-use $U4$ by 51%, 64 $\times$ 64 MIMO DL NOMA with C-CH CCRN enhanced SE performance by 64%, and 64 $\times$ 64 MIMO DL NOMA with D-CH CCRN boosted performance by 65% SE compared to SISO DL NOMA at 40 dB transmit power. While 128 $\times$ 128 M-MIMO DL NOMA improved SE performance for the best $U4$ user by 79%, 128 $\times$ 128 M-MIMO DL NOMA with C-CH CCRN boosted SE performance by 85%, and 128 $\times$ 128 M-MIMO DL NOMA with D-CH CCRN enhanced SE performance by 86% when compared to SISO DL NOMA SE performance at 40 dB transmit power. We discovered that the second proposed method, when using D-CH with CCR-NOMA, produced the best SE performance for users. On the other hand, the spectral efficiency is significantly increased when applying MIMO and M-MIMO techniques.

Keywords: non-orthogonal multiple access (NOMA); multiple-input multiple-output (MIMO); massive MIMO (M-MIMO); cooperative cognitive radio (CCR)

Citation: Hassan, M.; Singh, M.; Hamid, K.; Saeed, R.; Abdelhaq, M.; Alsaqour, R.; Odeh, N. Enhancing NOMA's Spectrum Efficiency in a 5G Network through Cooperative Spectrum Sharing. *Electronics* **2023**, *12*, 815. https://doi.org/10.3390/electronics12040815

Academic Editors: Jaime Lloret and Joel J. P. C. Rodrigues

Received: 14 January 2023
Revised: 31 January 2023
Accepted: 3 February 2023
Published: 6 February 2023

1. Introduction

Non-orthogonal multiple access (NOMA) has long been considered an important enabling technology for next-generation wireless networks. NOMA can improve the overall spectrum efficiency (SE) of the system and provide better fairness to serving users [1,2]. Using a superposition coding scheme, NOMA systems depend on the base station (BS) to assess the difference between signals from different users. The mobile terminal receivers can remove the intra-beam interference by using a technique called successive interference cancellation (SIC).

NOMA's primary tenet was articulated in [3], which can accommodate multiple users by splitting them by time or rate. It is important to note that, the more orthogonal resources available, the more NOMA users there are [4–6]. There are two main NOMA domains: (1) the NOMA power domain (PD) and (2) the NOMA code domain (CD). Many users with varying power transmissions use the same frequency or time resource in the first category. For the second group, the codebook with the data matched the design of the codebook for each user [7]. As a result, the capacity and SE of future systems will have to be dramatically improved to deal with the expected increase in traffic. The next generations of mobile networks will greatly increase resource utilization and system capacity [8]. One way to achieve this is by sharing the spectrum (both in time and space) among multiple users. With non-orthogonal allocation, NOMA can accommodate more users than the number of orthogonal resource modules.

Unfortunately, the frequency band that can be used in wireless applications is limited. Therefore, it is vital to develop new techniques to meet the increasing traffic and service requirements and overcome the eventual spectrum failure [9]. The use of a cognitive radio (CR) is a well-known method that can help with spectrum shortages [10]. There are primary users (PUs) and secondary users (SUs) in the CR network, wherein the SUs can broadcast over primary spectrum bands if interference from PUs is acceptable.

The authors in [11] examined an essential CR process. Two methods of achieving spectrum sharing that allows for greater utilization of radio frequencies are discussed. These methods aim to avoid interference between simple and cognitive radio licenses. According to [12]'s spectrum utilization situation, it is possible to categorize the various forms of spectrum access. In terms of spectrum use, it is possible to sort the different types of spectrum access studied in [13] into groups. Multiple-input and multiple-output (MIMO) NOMA technology is used for primary and secondary users to achieve active cooperative spectrum sensing (CSS) in a cognitive radio network (CRN). The CRN's capacity is enhanced between the additive white Gaussian noise (AWGN) and Rayleigh fading channels. However, the ways of accessing CRN have not been clarified, and the number of users is modest. Moreover, the obtained results cannot be generalized to a large network, and the effect of the power location coefficients is not mentioned [14].

The primary contribution of this work is to, when the primary user experiences channel unavailability or instability, activate the cooperative cognitive radio (CCR) in the same network and in a single cell in 5G through the competing channel (C-CH) or a dedicated channel (D-CH). This results in increased throughput and system efficiency. The following are some of the other important contributions made by the current work:

In the 5G network, DL PD NOMA was integrated with CCR in two different ways: with single-input, single-output (SISO) and MIMO (multiple-input, multiple-output) and MIMO (massive-input, multiple-output).

It has been demonstrated that the proposed model integration enhances SE when compared to SISO DL NOMA (conventional model).

Establishing a quantitative measure for the degree to which the proposed methods are used improves performance while utilizing a variety of design parameters.

The following presentation is used in the remaining sections of the paper: Previous and related works are discussed in Section 2. The proposed mathematical model for the system is discussed in Section 3. Section 4 reveals the simulation and results, and Section 5 concludes the study with a consideration of possible future research directions.

2. Related Work

The author of [15] analyzed the CR-NOMA system's outage probability (OP) and throughput. Closed expressions of OP were constructed to evaluate secondary network users' performance with primary network interference. Numerical findings indicate that correct power distribution and energy harvesting parameters can assure equitable performance for both users. The author verified the spectral structure of the MIMO-CR-NOMA internet of things (IoTs) frameworks, as well as calculated the throughput per user and the overall throughput. In [16], the frame rate was calculated for CR-OMA, CR-NOMA, CR-MIMO, and MIMO-CR-NOMA., with negative conditions such as optimal channel condition and a linear channel.

The author has formulated and addressed a problem to improve productivity in a multi-carrier NOMA system. Using a CRN base in a multi-carrier NOMA network increases the total system throughput at a modest PU throughput loss rate without exceeding the base target rate [17].

The author found asymptotic expressions for a NOMA-based, overlaid CRN for Industry 5.0 [18] with the help of OP analytical expressions and the ergodic rate for primary and secondary users.

The impacts of capacitance, phase, and power distribution on system performance are explored via simulation. For multi-carrier NOMA systems exposed to user fairness requirements, in [19], the author suggested a low-complexity resource allocation approach that offered a compromise between energy efficiency and spectrum efficiency. The proposed NOMA system produces higher energy efficiency (EE) and SE than state-of-the-art approaches, and does so with minimal complexity, as demonstrated by the numerical results. The NOMA cognitive system's interruption efficiency is examined in combination with an imperfect SIC. Closed models are used to determine how likely it is that the primary and secondary users will have outages, and simulations are used to ensure that the performance study results are corrected [20].

An active refracting reconfigurable intelligent surface (RIS)-based transmitter was investigated for the purpose of sending the confidential signal over an IoT network, while a passive reflective RIS was used to enhance the secrecy performance of users in the presence of multiple eavesdroppers. The simulated results prove the efficacy of the proposed design, which maximizes the weighted sum secrecy rate by coordinating the power allocation, transmit beamforming (BF), and phase shifts of the refracting and reflective RIS [21].

The author proposed a joint optimization design for the NOMA-based satellite–terrestrial integrated network (STIN), where a satellite multicast communication network shares the millimeter wave spectrum with a cellular network employing NOMA technology. The simulation results confirm the effectiveness and superiority of the proposed approach in comparison to existing approaches, assuming that the satellite uses a multibeam antenna array and the base station uses a uniform planar array [22].

The author explores secure energy efficient beamforming in multibeam satellite systems where an eavesdropper is present in each beam with an aim to maximize the system's secrecy energy efficiency (SEE) within the constraints of the total transmit power budget. Simulation results are provided to prove that the proposed scheme outperforms the benchmark schemes, unlike the existing schemes, which are much more complicated [23].

An active refracting RIS-based transmitter is investigated for sending the confidential signal over an IoT network, while a passive reflective RIS is used to enhance the secrecy performance of users in the presence of multiple eavesdroppers. Simulated results prove the efficacy of the proposed design, which maximizes the weighted sum secrecy rate by coordinating the power allocation, transmit beamforming (BF), and phase shifts of the refracting and reflective RIS [24].

For a large-scale, cell-free uplink MIMO system, the author presented a partial collaborative zero-impact decoding (PCZF) strategy, wherein neighboring access points (APs) around each user's equipment (UE) exchange CSI and work together to minimize interference via zero-effect decoding. The numerical findings verify the accuracy of the theoretical analysis and the efficacy of the suggested energy control algorithms after the analogy based optimization of the aggregation rate [25].

3. System Model

3.1. SIOS DL NOMA

The study was divided into three typical scenarios, each with three models, as depicted in the next sections. As shown in Figure 1, the SISO DL NONA system is considered (i.e., no multiple antenna elements). The NOMA system performs with and without adopting cooperative cognitive radio network (CCRN) integration for free and dedicated channels in the same network and single cell.

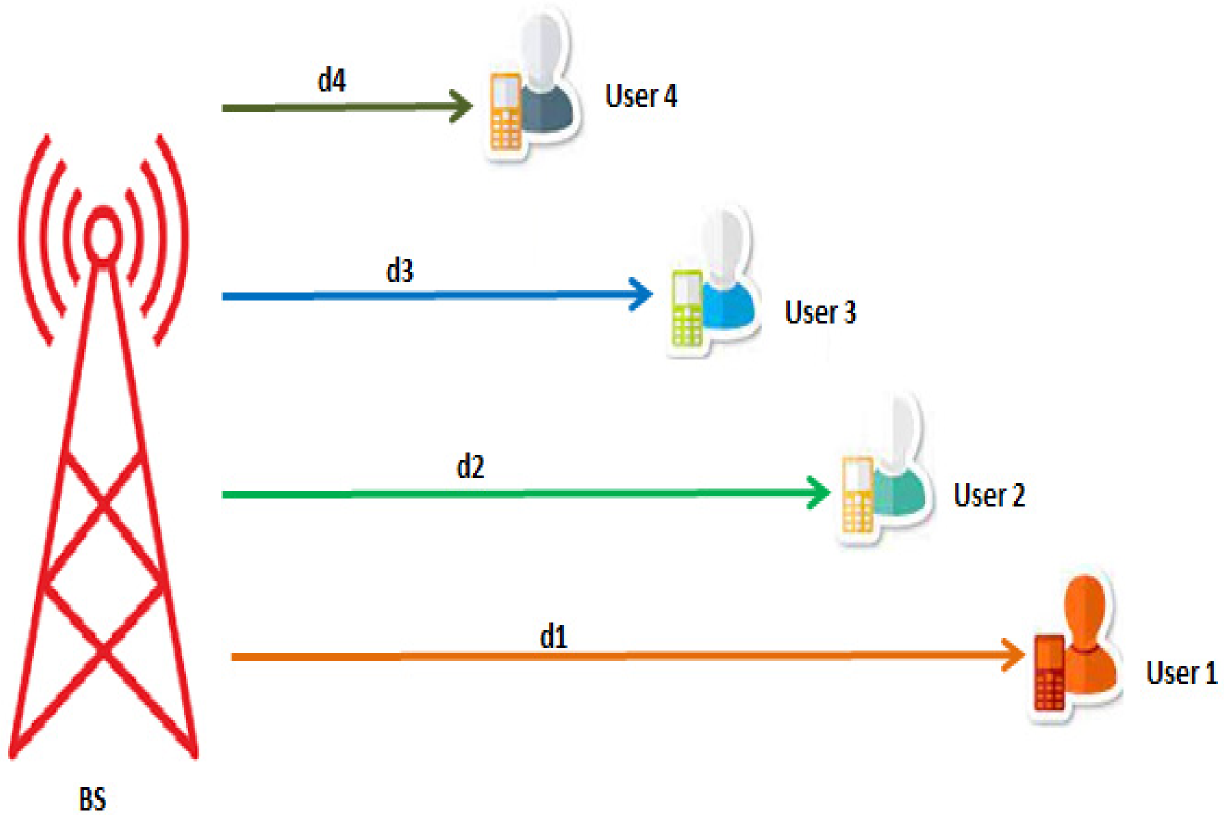

Figure 1. Depicts the wireless network with four users (DL-NOMA PD).

Suppose that the wireless network has four NOMA users $(U1,\ U2, U3,$ and $U4)$, each located a certain distance from the BS and denoted by $d1$, $d2$, $d3$, and $d4$, respectively. Note that, based on the users' location, $U1$ (who is located far away from the BS) is expected to receive a weaker signal compared to $U4$ (who is the closest to the BS). Let h_1, h_2, h_3, and h_4 represent the Rayleigh fading coefficients that they correspond to $|h_1|^2|h_2|^2|h_3|^2$. Their current power coefficients are denoted by $\alpha_1,\ \alpha_2,\ \alpha_3,$ and α_4, respectively.

The NOMA PD principles state that the user with a stronger signal (i.e., located close to the BS) should be allocated less power. In comparison, the user with a weaker signal (i.e., located far away from the BS) should be allocated more power. As a result, adjusted power coefficients are denoted by $x_1,\ x_2,\ x_3,$ and x_4. For simplicity, we use a set of power coefficients in this paper. To improve efficiency, several dynamic power coefficient strategies are available. Let the adjusted power coefficients $x_1,\ x_2,\ x_3,$ and x_4 exceed the quadrature phase-shift keying (QPSK) messages that will be sent to the base stations. The BS's encoded overlay signal can then be expressed as $x = \sqrt{p}(\sqrt{\alpha_1}x_1 + \sqrt{\alpha_2}x_2 + \sqrt{\alpha_3}x_3 + \sqrt{\alpha_4}x_4)$. The signal received by the ith user can be expressed as: $y_i = h_i x + n_i$, where n_i denotes AWGN experienced by the ith user (U_i).

The strongest signal is used to decode y_1 since it interacts directly with the other three signals. Achievable maximums are provided in [26,27].

$$R_1 = \log_2\left(1 + \frac{\alpha_1 P|h_1|^2}{\alpha_2 P|h_1|^2 + \alpha_3 P|h_1|^2 + \alpha_4 P|h_1|^2 + \sigma^2}\right) \tag{1}$$

After some manipulations, the achievable maximums produced in (1) can be written as:

$$R_1 = \log_2\left(1 + \frac{\alpha_1 P|h_1|^2}{(\alpha_2 + \alpha_3 + \alpha_4)P|h_1|^2 + \sigma^2}\right) \tag{2}$$

As illustrated in Equation (2), since the denominator is the sum of the power coefficients from the other three users ($\alpha_2 + \alpha_3 + \alpha_4$), this means that the power coefficient of the intended user (i.e., α_1) should satisfy the condition: $\alpha_1 > \alpha_2 + \alpha_3 + \alpha_4$. The power of the first user ($U1$) is then dominated by the transmitted signal x and the received signal y_1. Let us now write the equation for the second user ($U2$) rate. First, $U1'$s data must be removed and regarded as an interference, as $\alpha_2 < \alpha_1$, and $\alpha_2 > \alpha_3 > \alpha_4$ using SIC. After SIC deletes the $U1$ data, the achieved rate is $U2$.

$$R_3 = \log_2\left(1 + \frac{\alpha_3 P|h_3|^2}{\alpha_4 P|h_3|^2 + \sigma^2}\right) \tag{3}$$

Next, y_3, despite $U1$, $U2$, $U3$, and $U4$ ($\alpha_3 < \alpha_1$, $\alpha_3 < \alpha_2$), is in the denominator's overlapping term. Finally, canceled data y_3 required the execution of three SIC functions. Because α_1 prevails, it must be removed first. Following that, the α_3 term must be removed. Then, the achievable rate is written using:

$$R_3 = \log_2\left(1 + \frac{\alpha_3 P|h_3|^2}{\alpha_4 P|h_3|^2 + \sigma^2}\right) \tag{4}$$

The achieved y_4, illustrated as $U1$, $U2$, $U3$, and $U4$ ($\alpha_3 < \alpha_1$, $\alpha_3 < \alpha_2$, $\alpha_3 < \alpha_4$), is in the denominator's intersecting term. Eventually, removed data y_4 necessitates the implementation of two SIC functions. Because the α_1 reign is supreme, it must be deleted first. Following that, the α_3 term must be eliminated. The attainable rate was,

$$R_4 = \log_2\left(1 + \frac{\alpha_4 P|h_4|^2}{\sigma^2}\right) \tag{5}$$

3.1.1. CCRN-Based Free Channels

Assume the wireless network has four NOMA users ($U1$, $U2$, $U3$, and $U4$), where ($\alpha_3 < \alpha_1$, $\alpha_3 < \alpha_2$) and the cooperative cognitive radio (CCR) network is depicted as in Figure 2. Let us represent their respective BS distances d_1, d_2, d_3, and d_4. In terms of BS usage, $U1$ is the weaker/far user, while $U4$ is the stronger/near user. To represent the Rayleigh fading values, we can use the following formula:$|h_1|^2|h_2|^2|h_3|^2|h_4|^2$.

The CCR spectrum investigated the status of the channel and the possibility of using it for communication. Suppose the channel status is unstable and communication is weak. In that case, two options are related to the CCR channel status (available or not). When the CCR channel is available, NOMA can use it.

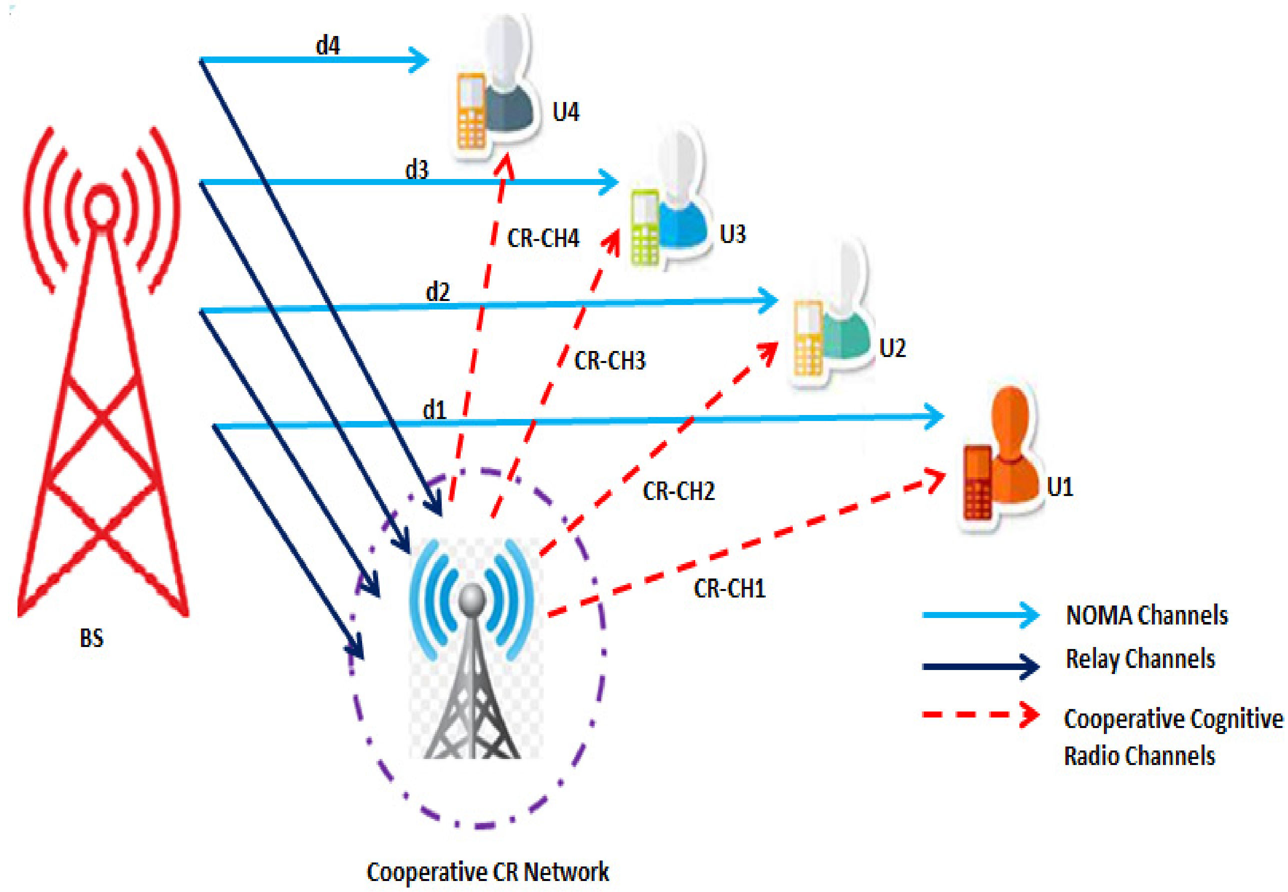

Figure 2. DL-NOMA PD with the CCR network with four users' system model.

CR must use the whole spectrum window to complete packet transmission (s). Assuming that T_{window} denotes such a spectrum window period, it is obvious that [28]:

$$T_{window} \geq T_{sense} + T_{CR} - Transmission + T_{ramp} - up + T_{ramp} - down \quad (6)$$

where T_{sense} denotes the minimum sensing and duration required to ensure the CR transmission opportunity and acquisition of related communication parameters, T_{CR} Transmission denotes the transmission period for CR packets, and T_{ramp} up/down denotes the transmission ramping (up or down) period. Figure 3 shows the CR transmission opportunity window when the beacon signals have fixed separation [29].

$$PD = \frac{Number\ of\ acquisitions}{Total\ number\ of\ opportunities} = \frac{Over\_Num}{NOP} \quad (7)$$

Spectrum Sensing

To choose between the two hypotheses, spectrum sensing on link-level targets in a single primary system is used.

$$y[n] = \{w[n]\ h\ s[n] + w[n]\ n = 1\ldots\ N\ \frac{H_0}{H_1} \quad (8)$$

where $y[n]$ represents the complex signal received by the CR, $s[n]$ represents the primary user's transmitted signal, $w[n]$ represents AWGN, h represents the complex gain of an ideal channel, and N represents the observation interval. If the channel is not perfect, h and $s[n]$ are convolved rather than multiplied. H_0 denotes the null hypothesis that no primary user is present. In contrast, H_1 denotes the alternate hypothesis that a primary user signal exists. Spectrum sensing techniques were divided into two categories: energy based and feature-based [30].

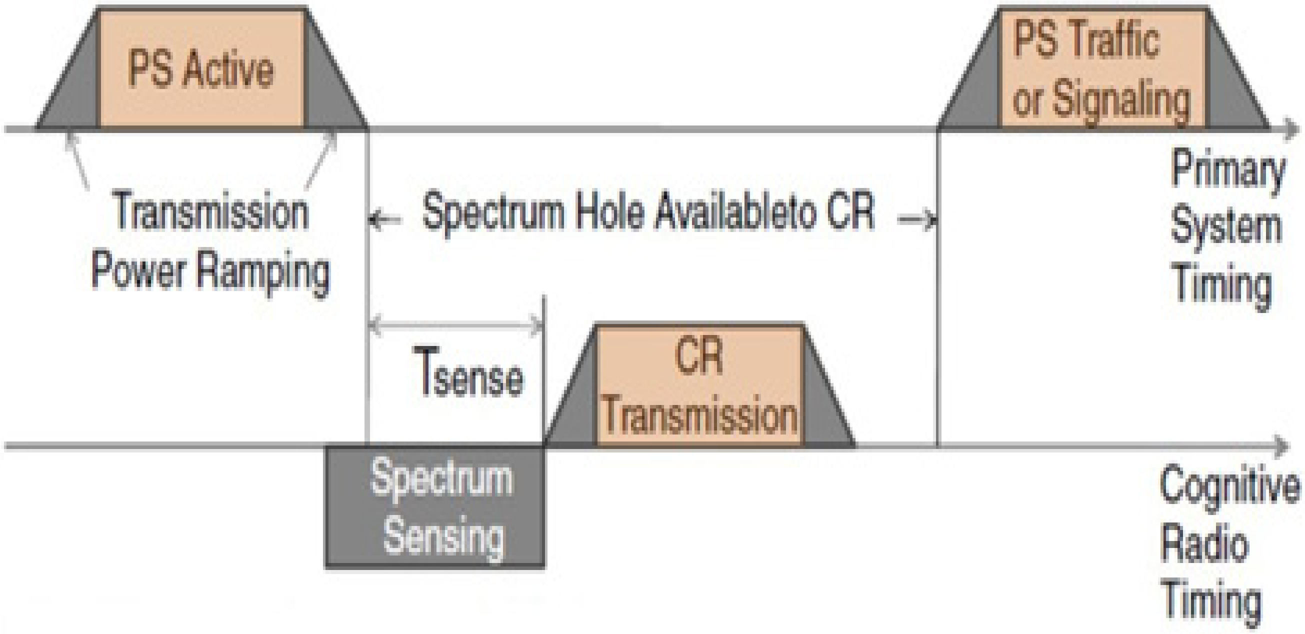

Figure 3. The window of opportunity for CR transmission.

Energy Detection

Over the observation interval, the received signal is squared and integrated. The integrator's output is then compared to a threshold to determine whether the primary user exists. In other words, the following binary choice is made:

$$\begin{cases} H_0,\ if\ \sum_{n=1}^{N} \left| y[n]^2 \right| \leq \lambda \\ \quad H_1,\ otherwise \end{cases} \tag{9}$$

where λ is the threshold that is affected by the receiver noise.

$$PF = P\left(\frac{H_1}{H_0}\right) = P\left(\frac{PU}{H_0}\right) = P\left(\frac{y_n}{H_0}\right) = 1 - F_{H_0}(Th) \tag{10}$$

False alarm probability and F_{H_0} represent the cumulative distribution function (CDF) [31].

$$PD = \frac{Number\ of\ acquisitions}{Total\ number\ of\ opportunities} = \frac{Over\_Num}{NOP} \tag{11}$$

$$PD = 1 - P_M \ = 1 - P\left(\frac{H_0}{H_1}\right) \tag{12}$$

$$PD = \left[e^{\frac{-Th}{2}} * \frac{1}{n!}\left(\frac{Th}{2}\right)^n\right] + \left[e^{\frac{-Th}{2(1+L)}} * \left(\frac{1+L}{L}\right)\right] - \left[e^{\frac{-Th}{2}} * \frac{1}{n!} * \frac{Th * L}{2(1+L)}\right] \tag{13}$$

$$Pm = 1 - PD \tag{14}$$

where PD represents the detection probability and Th is the threshold and L is the SNR; P_M represents the probability of missed detection and P_{FA} is the false-alarm probability [32].

The probability of error,

$$P_e = P_F * P_{(H_0)} + P_M riP_{(H_1)} \tag{15}$$

3.1.2. CCR-Based Dedicated Channel

The CCR examined the state of the channel and how it could be used for communication when a primary communication system is running and when the channel state is unstable or communication is weak. In this case, there is only one condition in which the CCR channel is available (high priority), and NOMA users can use it (see Figure 2).

3.2. MIMO DL PD NOMA

Consider 64 × 64 MIMO DL NOMA PD, 64 × 64 MIMO DL NOMA PD with CCRN C-CH, and 64 × 64 MIMO DL NOMA PD with CCRN D-CH under the assumption that there are N users, $U1,\ U2,\ U3, \ldots, U_N$ ($\alpha_2 < \alpha_1,\ \alpha_3 < \alpha_2,\ \alpha_4 < \alpha_2$) in a single cell in the 5G network.

$$x = \sqrt{P}(\sqrt{\alpha_1}x_1 + \sqrt{\alpha_2}x_2 + \sqrt{\alpha_3}x_3 + \sqrt{\alpha_4}x_4) \tag{16}$$

where α are the NOMA power allocation coefficients [33]. The transmit antennas all broadcast x simultaneously. From this, we know what U_N is detecting as a signal:

$$y_N = xh_{N1} + xh_{N2} + \ldots + xh_{NN} \tag{17}$$

where n_N is the total number of samples from the AWGN with a zero-mean and σ^2 variation and N is the number of users [34]. For each user, we can calculate their Rayleigh fading channel as:

$$h_{ik} = \sum_{i=1}^{k} h_{ik} \tag{18}$$

Where $i = 1, 2, 3, 4$ is the number of users; $k = 64$ is the total number of available channels. Moreover, the signal is received by the BS.

$$y = \sqrt{P_{x1}}h_{1N} + \sqrt{P_{x2}}h_{2N} + \sqrt{P_{x3}}h_{3N} + \sqrt{P_{x4}}h_{4N} \tag{19}$$

To analyze the channel's state and its possibilities for communication, we used the same model, with the CCR spectrum included. Suppose the channel state is unstable and communication is poor. In that case, the state of the CCR channel provides two possibilities: C-CH or D-CH [35].

3.3. Massive MIMO DL PD NOMA

Regarding 128 × 128 M-MIMO DL NOMA PD, 128 × 128 M-MIMO DL NOMA PD with a CCRN competitive channel (C-CH), and 128 × 128 M-MIMO DL NOMA PD with a CCRN dedicated channel (D-CH), in this section, we assume that the wireless network has four users, represented by $U1,\ U2,\ U3, UN4$ ($\alpha_2 < \alpha_1,\ \alpha_3 < \alpha_2,\ < \alpha_4 < \alpha_3$), located at varying distances from one another and all using the 128 × 128 M-MIMO DL NOMA PD under the same conditions as before.

We employ the same methodology to evaluate the channel's current accuracy and viability as a communication medium. Users with NOMA can use the CR channel if it becomes operational. Here, we maintain the same basic idea, wherein NOMA users can tune into the CCR frequency on a significant priority [36]. For each user, we can calculate their Rayleigh fading channel as:

$$h_{jM} = \sum_{j=1}^{M} h_{jM} \tag{20}$$

where $j = 1, 2, 3, 4$ is the number of users; $M = 128$ is the total number of available channels.

4. Numerical Simulation and Results

The DL NOMA PD in 5G networks employing MIMO and M-MIMO was developed in MATLAB, along with the system model and simulator settings for those technologies. Table 1 shows an accurate consideration of the simulation parameters.

Table 1. Simulator parameters for the DL scenario.

No.	Parameters	Values	
1.	Number of users	4 users	
2.	Transmit power	0 to 30 dBm	
3.	Bandwidth	BW	80 MHz
4.	Distances	$U1$	900 m
		$U2$	700 m
		$U3$	400 m
		$U4$	200 m
5.	Power coefficients	$U1$	0.75
		$U2$	0.188
		$U3$	0.047
		$U4$	0.011
6.	Path loss exponent	4	
7.	SISO	1×1	
8.	MIMO	64×64	
9.	M-MIMO	128×128	
10.	Modulation	QPSK	

Based on the software's execution in the three scenarios, the following figures displayed SE evaluation versus transmit power for DL NOMA PD and CCRN with SISO, with 64×64 MIMO and 128×128 M-MIMO in same network and single cell [37].

4.1. SISO DL NOMA PD

For SISO DL NOMA PD with an unstable channel state, Figure 4 depicted the SE vs. transmit power of four users $U1$, $U2$, $U3$, and $U4$ in distances of 900 m, 700 m, 400 m, and 200 m, with power location coefficients of 0.75, 0.188, 0.047, and 0.011, respectively. According to the findings, the SE increased as the transmit power increased. The best result of SE is 3.9 bps/Hz/cell at a transmitting power of 30 dBm for $U4$, who was physically closest to the BS, followed by $U3$, $U2$, and finally $U1$.

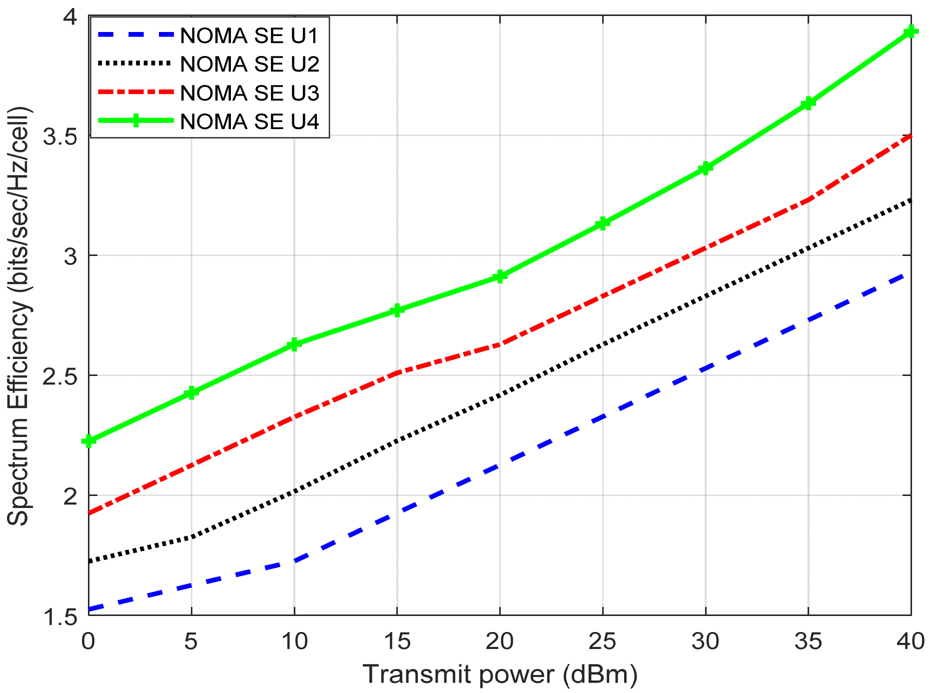

Figure 4. SE vs. transmitting power for 4 users SISO DL NOMA PD.

Figure 5 shows SE against transmitting power for four users with different distances and power location coefficients for SISO DL NOMA PD combined with the CCRN with the C-CH free channel (first model). The highest SE outcome is 5.09 bps/Hz/cell for *U*4, at a transmit power of 30 dBm.

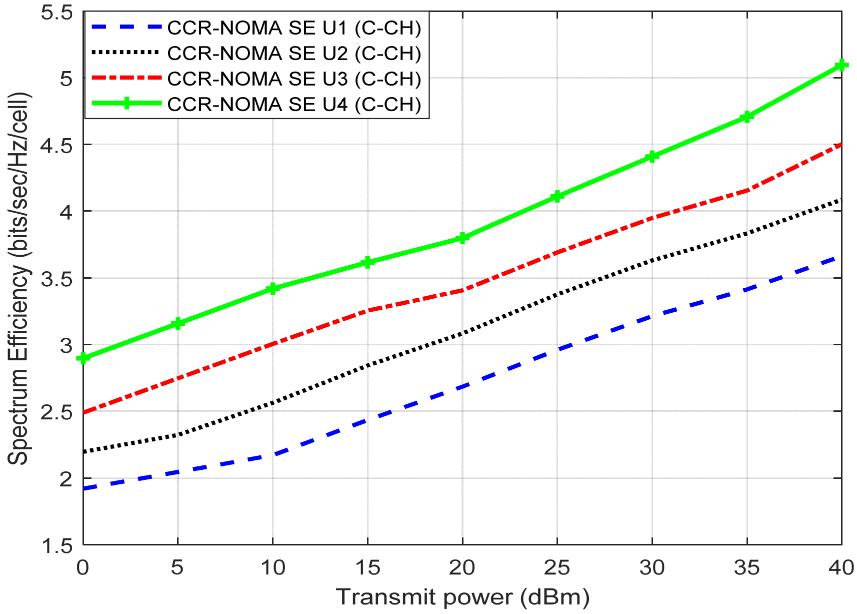

Figure 5. SE against transmitting power for 4 users' SISO DL NOMA PD with C-CH CCRN.

For SISO DL NOMA PD integrated with the CCRN with the D-CH (dedicated channel second model), the SE versus transmit power is demonstrated in Figure 6 for four users with various distances and power location coefficients. The greatest SE result is 7.2 bps/Hz/cell for *U*4, at a transmit power of 30 dBm.

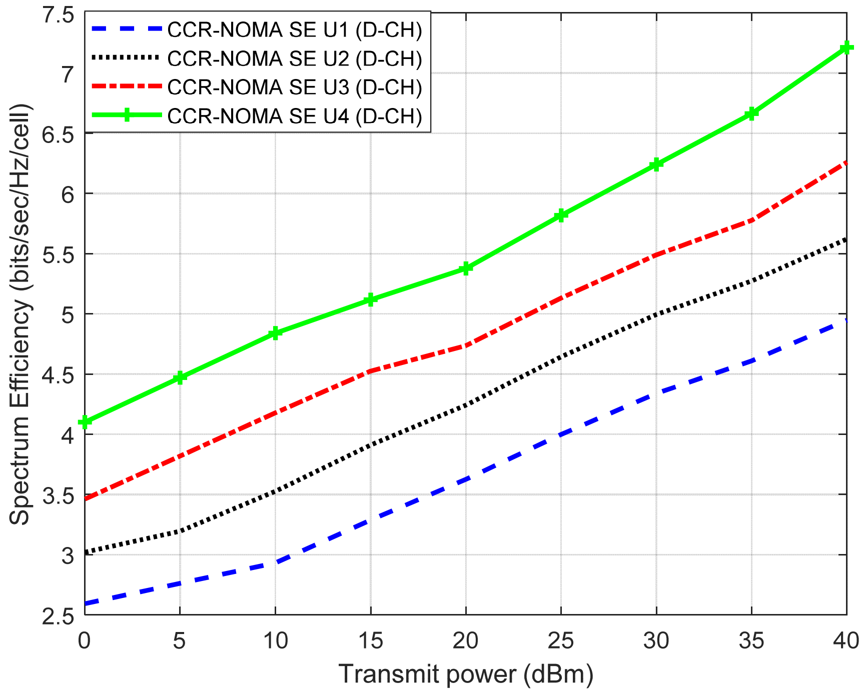

Figure 6. SE versus transmitting power for 4 users' SISO DL NOMA PD with D-CH CCRN.

4.2. MIMO DL-NOMA PD

Figure 7 exhibited 64 × 64 MIMO DL NOMA PD with an unstable channel state SE vs. the transmit power result of four users ($U1$, $U2$, $U3$, and $U4$) at distances of 800 m, 600 m, 300 m, and 100 m, with power location coefficients of 0.6, 0.3, 0.075, and 0.01875, accordingly. Increases in transmit power are reflected in a proportional rise in SE. The nearest user to the BS $U4$ has the best SE values of 12.23 bps/Hz/cell, followed by $U3$, $U2$, and $U1$ at a transmitting power of 40 dBm. After adopting 64 × 64 MIMO technology with NOMA, the best user, $U4$, boosted the SE by 8.33 bps/Hz/cell at a transmission power of 40 dBm when compared with the SISO DL NOMA PD.

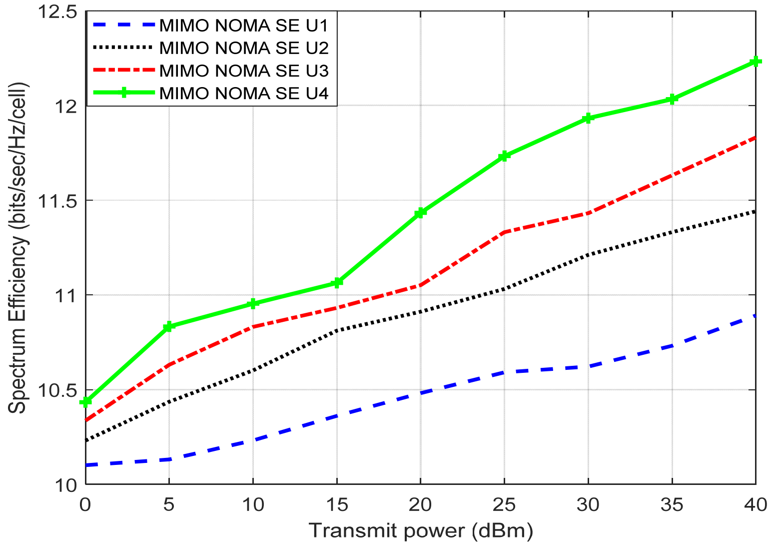

Figure 7. SE vs. transmitting power for 4 users' 64 × 64 MIMO DL-NOMA PD.

Figure 8 depicted the SE against the transmit power for four users with varied distances and power location coefficients, using a 64 × 64 MIMO DL NOMA PD integrated with the CCRN for the C-CH. The nearest user to the BS $U4$ has the highest SE performance of 17.75 bps/Hz/cell at a transmitting power of 40 dBm. After implementing 64 × 64 MIMO technology with CCRN NOMA (C-CH), the best user, $U4$, improved the SE by 12.66 bps/Hz/cell at a transmitting power of 40 dBm when compared with the SISO DL CCR-NOMA PD for the C-CH.

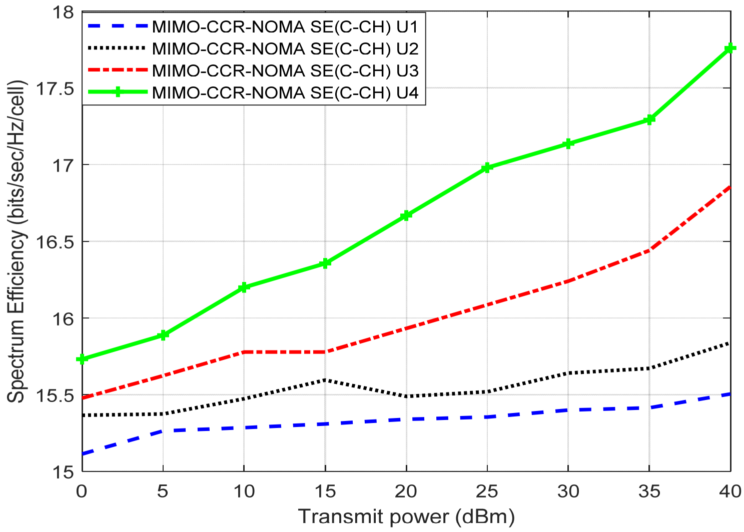

Figure 8. SE against transmitting power for 4 users' 64 × 64 MIMO DL-NOMA PD with C-CH CCRN.

Four users with varied distances and power location coefficients are displayed in Figure 9, exhibiting SE vs. transmit power for a 64 × 64 MIMO DL NOMA PD in connection with the CCRN for the D-CH. The user nearest to the BS, *U*4, has the greatest SE performance of 18.51 bps/Hz/cell at a transmitting power of 40 dBm. When analyzing the performance of the best user, *U*4, and after applying 64 × 64 MIMO technology with CCRN NOMA with C-CH, the SE was enhanced by 11.31 bps/Hz/cell at a transmitting power of 40 dBm when compared with the SISO DL CCR-NOMA PD for the D-CH. The results obtained are more significant than the SE performance in reference [38].

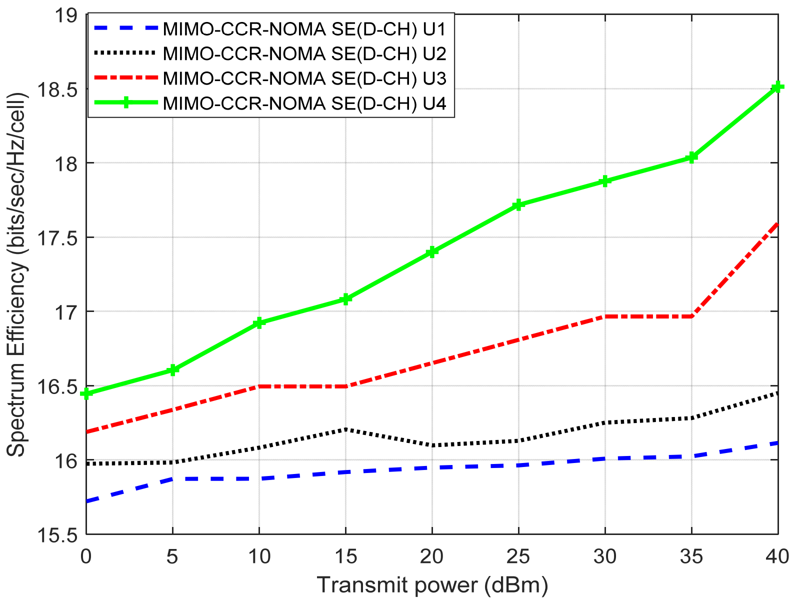

Figure 9. SE versus transmitting power for 4 users' 64 × 64 MIMO DL-NOMA PD with D-CH CCRN.

4.3. M-MIMO DL NOMA PD

Figure 10 depicts the SE versus transmit power for four users (*U*1, *U*2, *U*3, and *U*4) in the 128 × 128 M-MIMO DL NOMA PD at varying distances and power location coefficients. A higher transmit power typically results in higher SE. *U*4, the user closest to the BS, has the best SE performance at 40 dBm of 33.89 bps/Hz/cell, followed by *U*3, *U*2, and *U*1. When 128 × 128 M-MIMO technology with NOMA was used, the best user, *U*4, saw an increase of 29.99 bps/Hz/cell in SE at 40 dBm transmit power compared to the SISO DL NOMA PD.

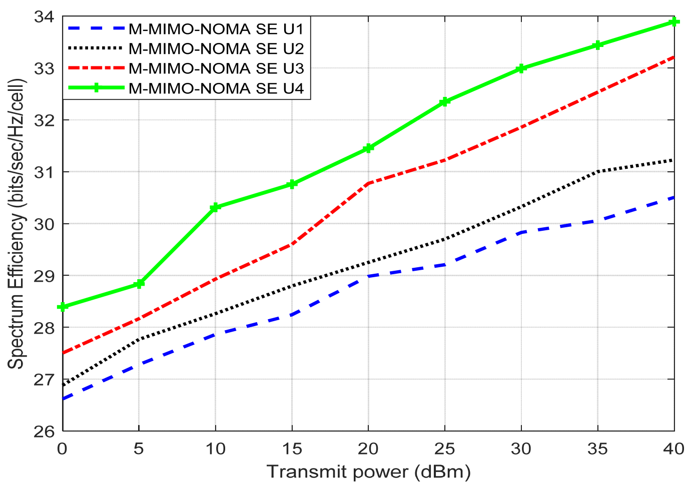

Figure 10. SE vs. transmitting power for 4 users' 128 × 128 M-MIMO DL NOMA PD.

Figure 11 shows SE vs. transmit power for 128 × 128, DL, NOMA, and PD integration, with the CCRN using C-CH. At 40 dBm of transmit power, the SE performance of *U*4, who is physically closest to the BS, is the best, at 50.12 bps/Hz/cell, when compared to the SISO DL CCR-NOMA PD for the C-CH; moreover, the SE was improved by 45.03 bits/s/Hz/cell after installing 128 × 128 M-MIMO technology with NOMA.

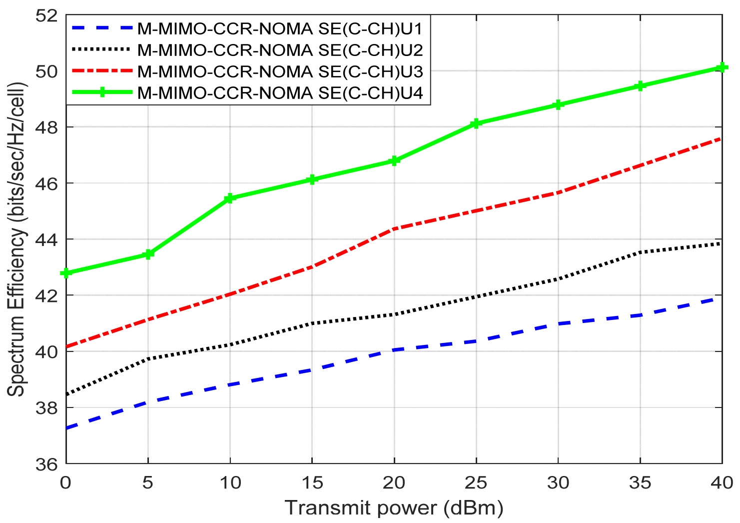

Figure 11. SE against transmitting power for 4 users' 128 × 128 M-MIMO DL NOMA PD with C-CH CCRN.

Figure 12 depicts the M-MIMO DL NOMA PD paired with the CCRN D-CH, showing the SE versus transmitting power for four users at different distances and power location factors. At a transmission level of 40 dBm, *U*4, the user closest to the BS, achieved the best SE performance, at 53.29 bps/Hz/cell. Comparing *U*4's SE improvement with the SISO DL CCR-NOMA PD for the D-CH, the SE was improved by 46.09 bps/Hz/cell at 40 dBm after employing 128 × 128 M-MIMO technology with NOMA. These findings are more substantial than the SE performance in reported other works.

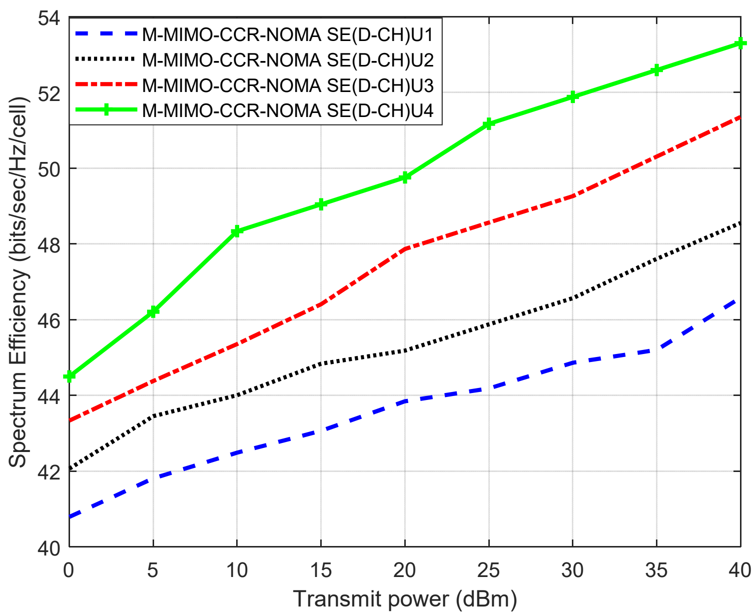

Figure 12. SE versus transmitting power for 4 users' 128 × 128 M-MIMO DL NOMA PD with D-CH CCRN.

5. Conclusions

This paper demonstrated the SE performances of DL NOMA PDs in a 5G network combined with SISO, 64 × 64 MIMO, and 128 × 128 M-MIMO technologies integrated with the CCRN in two novel ways: the first method allowed users to access CCRN channels through the competition channel (C-CH), and the second method permitted the CCRN to meet any of the channel needs of users via the dedicated channel (D-CH), with all users varying in different distances, PLCs, and transmit power. In particular, the performance evaluation considered the SIC, unstable channels, and AWGN under Rayleigh fading. The DL NOMA system results showed that 64 × 64 MIMO and 128 × 128 M-MIMO integrated in the same network and in a single cell, with CCRN, significantly improved SE performance. The results indicated that the best SE performance for the user $U4$ is 3.9 bps/Hz/cell for SISO DL NOMA, 5.1 bps/Hz/cell for SISO DL NOMA with the CCRN with C-CH, and 7.2 bps/Hz/cell for SISO DL NOMA with the CCRN with D-CH at a 40 dBm transmit power. Moreover, DL 64 × 64 MIMO NOMA most effectively enhanced SE performance for $U4$ by 51%, 64 × 64 MIMO DL NOMA with CCRN (C-CH) improved the SE performance by 64%, while 64 × 64 MIMO DL NOMA with CCRN (D-CH) enhanced the SE performance by 65% at a 40 dBm transmit power when compared to the SE performance of SISO DL NOMA. While DL 128 × 128 M-MIMO NOMA improved SE performance for the best user, $U4$, by 79%, 128 × 128 M-MIMO DL NOMA with CCRN (C-CH) enhanced the SE performance by 85%, and 128 × 128 M-MIMO DL NOMA with CCRN (D-CH) improved it by 86% at a 40 dBm transmit power, when compared to SISO DL NOMA's SE performance. The combination of the SISO 64 × 64 MIMO and 128 × 128 M-MIMO DL NOMA systems with CCRN considerably improved SE.

From the results, the main ways to improve SE are to add more users and use M-MIMO, as well as to use efficient channel coding methods, effective bandwidth shaping methods, and massive multiple access methods. A future study target is the exploration of a combination between massive MIMO cooperative NOMA and cognitive radio for uplink.

Author Contributions: Conceptualization, M.H.; methodology, M.H. and M.S.; software, M.H.; validation, M.H., M.S., N.O. and K.H.; formal analysis, M.H., M.S. and K.H.; investigation, R.S., R.A. and N.O.; resources, R.S., M.A. and R.A.; data curation, R.S., M.A., N.O. and R.A.; writing—original draft, M.H.; writing—review and editing, M.A., R.S. and R.A.; visualization, M.H. and K.H.; supervision, M.S.; project administration, M.S.; funding acquisition, M.A. All authors have read and agreed to the published version of the manuscript.

Funding: This work is funding by the Deanship of Scientific Research, Kingdom of Saudi Arabia, Umm Al-Qura University, Makkah. Under Grant Number: 22UQU4281755DSR03. In addition, this research was supported by the Princess Nourah bint Abdulrahman University Researchers Supporting Project Number (PNURSP2023R97), Princess Nourah bint Abdulrahman University, Riyadh, Saudi Arabia.

Data Availability Statement: Not applicable.

Acknowledgments: Princess Nourah bint Abdulrahman University Researchers Supporting Project Number (PNURSP2023R97), Princess Nourah bint Abdulrahman University, Riyadh, Saudi Arabia.

Conflicts of Interest: The authors declare no conflict of interest.

References

1. Ding, Z.; Lei, X.; Karagiannidis, G.; Schober, R. A Survey on Non-Orthogonal Multiple Access For 5g Networks: Research Challenges and Future Trends. *IEEE J. Sel. Areas Commun.* **2017**, *35*, 2181–2195. [CrossRef]
2. Hassan, M.; Singh, M.; Hamid, K. Review of NOMA with Spectrum Sharing Technique. In *ICT with Intelligent Applications. Smart Innovation; Systems and Technologies*; Senjyu, T., Mahalle, P.N., Perumal, T., Joshi, A., Eds.; Springer: Singapore, 2022; Volume 248.
3. Ding, Z. Application of Non-Orthogonal Multiple Access in LTE and 5G Networks. *IEEE Commun. Mag.* **2017**, *55*, 185–191. [CrossRef]
4. Hassan, M.; Singh, M.; Hamid, K. Survey on NOMA and Spectrum Sharing Techniques in 5G. In Proceedings of the IEEE International Conference on Smart Information Systems and Technologies (SIST), Nur-Sultan, Kazakhstan, 28–30 April 2021; pp. 1–4.

5. Dai, L.; Wang, B.; Ding, Z. A Survey of Non-Orthogonal Multiple Access For 5G. *IEEE Commun. Surv. Tutor.* **2018**, *20*, 2294–2323. [CrossRef]
6. Makki, B.; Chitti, K.; Behravan, A.; Alouini, M. A Survey of Noma: Current Status and Open Research Challenges. *IEEE Open J. Commun. Soc.* **2020**, *1*, 179–189. [CrossRef]
7. Balasubramanya, N.; Gupta, A.; Sellathurai, M. Combining Code-Domain and Power-Domain NOMA for Supporting Higher Number of Users. In Proceedings of the IEEE Global Communications Conference (GLOBECOM), Abu Dhabi, United Arab Emirates, 9–13 December 2018; pp. 1–6.
8. Marcano, A.; Christiansen, H. A Novel Method for Improving the Capacity in 5G Mobile Networks Combining NOMA and OMA. In Proceedings of the IEEE 85th Vehicular Technology Conference (VTC Spring), Sydney, Australia, 4–7 June 2017.
9. Arzykulov, S.; Nauryzbayev, G.; Tsiftsis, T. Error Performance of Wireless Powered Cognitive Relay Networks with Interference Alignment. In Proceedings of the IEEE 28th Annual International Symposium on Personal, Indoor, and Mobile Radio Communications (PIMRC), Montreal, QC, Canada, 8–13 October 2017; pp. 1–5.
10. Arzykulov, S.; Tsiftsis, T.; Nauryzbayev, K. Outage Performance of Underlay CR-Noma Networks with Detect-and-Forward Relaying. In Proceedings of the IEEE Global Communications Conference (GLOBECOM), Abu Dhabi, United Arab Emirates, 9–13 December 2018; pp. 1–6.
11. Hassan, M.; Singh, M.; Hamid, K. Overview of Cognitive Radio Networks. *J. Phys. Conf. Ser.* **2020**, *1831*, 012013. [CrossRef]
12. Hu, F.; Zhu, K. Full Spectrum Sharing in Cognitive Radio Networks Toward 5g: A Survey. *IEEE Access* **2018**, *6*, 15754–15776. [CrossRef]
13. Hassan, M.; Singh, M.; Hamid, K. Survey on Advanced Spectrum Sharing Using Cognitive Radio Technique. *Adv. Intell. Syst. Comput.* **2021**, *1270*, 639–647.
14. Balachander, T.; Krishnan, T. Efficient Utilization of Cooperative Spectrum Sensing (CSS) In Cognitive Radio Network (CRN) Using Non-Orthogonal Multiple Access (Noma). *Wirel. Pers Commun* **2021**, *127*, 2189–2210. [CrossRef]
15. Do, D.-T.; Le, A.-T.; Lee, B.M. NOMA In Cooperative Underlay Cognitive Radio Networks Under Imperfect Sic. *IEEE Access* **2020**, *8*, 86180–86195. [CrossRef]
16. Thakur, P.; Singh, G. Spectral Efficient Designs of MIMO-Based CR-NOMA For Internet of Things Networks. *Int. J. Commun. Syst.* **2021**, *34*, 4888–4900. [CrossRef]
17. Manimekalai, T.; Romera, S.; Laxmikandan, T. Throughput Maximization for Underlay CR Multicarrier NOMA Network with Cooperative Communication. *ETRI J.* **2020**, *42*, 846–858. [CrossRef]
18. Li, X.; Gao, X.; Shaikh, S.; Ming, Z.; Huang, G. NOMA-Based Cognitive Radio Network with Hybrid FD/HD Relay in Industry 5.0. *J. King Saud Univ.* **2022**, 1319–1578. [CrossRef]
19. Zuo, Y.; Zhu, X.; Jiang, Y.; Wei, Z.; Zeng, H.; Wang, T. Energy Efficiency and Spectral Efficiency Tradeoff for Multicarrier Noma Systems with User Fairness. In Proceedings of the IEEE/CIC International Conference on Communications in China (ICCC), Beijing, China, 16–18 August 2018; pp. 666–670.
20. Tang, K.; Liao, S. Outage Analysis of Relay-Assisted Noma in Cooperative Cognitive Radio Networks with Swipt. *Information* **2020**, *11*, 500. [CrossRef]
21. Lin, Z.; Niu, H.; An, K.; Wang, Y.; Zheng, G.; Chatzinotas, S.; Hu, Y. Refracting RIS-Aided Hybrid Satellite-Terrestrial Relay Networks: Joint Beamforming Design and Optimization. *IEEE Trans. Aerosp. Electron. Syst.* **2022**, *58*, 3717–3724. [CrossRef]
22. Lin, Z.; Lin, M.; Wang, J.B.; de Cola, T.; Wang, J. Joint Beamforming and Power Allocation for Satellite-Terrestrial Integrated Networks With Non-Orthogonal Multiple Access. *IEEE J. Sel. Top. Signal Process.* **2019**, *13*, 657–670. [CrossRef]
23. Lin, Z.; An, K.; Niu, H.; Hu, Y.; Chatzinotas, S.; Zheng, G.; Wang, J. SLNR-based Secure Energy Efficient Beamforming in Multibeam Satellite Systems. *IEEE Trans. Aerosp. Electron. Syst.* **2022**, 1–4. [CrossRef]
24. Niu, H.; Lin, Z.; Chu, Z.; Zhu, Z.; Xiao, P.; Nguyen, H.X.; Lee, I.; Al-Dhahir, N. Joint Beamforming Design for Secure RIS-Assisted IoT Networks. *IEEE Internet Things J.* **2023**, *10*, 1628–1641. [CrossRef]
25. Wang, X.; Cheng, J.; Zhai, C.; Ashikhmin, A. Partial Cooperative Zero-Forcing Decoding for Uplink Cell-Free Massive MIMO. *IEEE Internet Things J.* **2022**, *9*, 10327–10339. [CrossRef]
26. Gamal, S.; Rihan, M.; Hussin, S.; Zaghloul, A.; Salem, A.A. Multiple Access in Cognitive Radio Networks: From Orthogonal and Non-Orthogonal to Rate-Splitting. *IEEE Access* **2021**, *9*, 95569–95584. [CrossRef]
27. Hamdi, M. Downlink Scheduling in 5G Massive MIMO. *J. Eng. Appl. Sci.* **2018**, *13*, 1376–1381.
28. Hassan, M.; Singh, M.; Hamid, K. BER Performance of NOMA Downlink for AWGN and Rayleigh Fading Channels In (Sic). *EAI Endorsed Trans. Mob. Com. Appl.* **2022**, *7*. [CrossRef]
29. Dinh, S.; Liu, H.; Ouyang, F. Massive MIMO Cognitive Cooperative Relaying. In *Wireless Algorithms, Systems, and Applications. WASA. Lecture Notes in Computer Science*; Biagioni, E., Zheng, Y., Cheng, S., Eds.; Springer: Berlin/Heidelberg, Germany, 2019; Volume 11604.
30. Chen, K.; Prasad, R. *Cognitive Radio Networks*, 1st ed.; Wiley & Sons: Hoboken, NJ, USA, 2009; pp. 183–216.
31. Hassan, M.; Singh, M.; Hamid, K.; Saeed, R.; Abdelhaq, M.; Alsaqour, R. Modeling of Noma-MIMO-Based Power Domain for 5g Network Under Selective Rayleigh Fading Channels. *Energies* **2022**, *15*, 5668. [CrossRef]
32. Liu, Y.; Pan, G.; Zhang, H.; Song, M. On the Capacity Comparison Between MIMO-NOMA and MIMO-OMA. *IEEE Access* **2016**, *4*, 2123–2129. [CrossRef]

33. Zeng, M.; Yadav, A.; Dobre, O.A.; Tsiropoulos, G.I.; Poor, H.V. Capacity Comparison Between MIMO-NOMA and MIMO-OMA With Multiple Users in a Cluster. *IEEE J. Sel. Areas Commun.* **2017**, *35*, 2413–2424. [CrossRef]
34. Amin, A.A.; Shin, S.Y. Capacity Analysis of Cooperative NOMA-OAM-MIMO Based Full-Duplex Relaying for 6G. *IEEE Wirel. Commun. Lett.* **2021**, *10*, 1395–1399. [CrossRef]
35. Shen, D.; Wei, C.; Zhou, X.; Wang, L.; Xu, C. Photon Counting Based Iterative Quantum Non-Orthogonal Multiple Access with Spatial Coupling. In Proceedings of the 2018 IEEE Global Communications Conference (GLOBECOM), Abu Dhabi, United Arab Emirates, 9–13 December 2018; pp. 1–6.
36. Hassan, M.B.; Ali, E.S.; Rashid, A. Ultra-Massive MIMO in THz Communications. In *Next Generation Wireless Terahertz Communication Networks*; CRC Group: Boca Raton, FL, USA; Taylor & Francis Group: London, UK, 2020. [CrossRef]
37. Rehman, B.U.; Babar, M.I.; Azim, G.A.; Amir, M.; Alhumyani, H.; Alzaidi, M.S.; Alshammari, M.; Saeed, R. Uplink power control scheme for spectral efficiency maximization in NOMA systems. *Alex. Eng. J.* **2023**, *64*, 667–677. [CrossRef]
38. Rehman, B.U.; Babar, M.I.; Ahmad, A.W.; Alhumyani, H.; Azim, G.A.; Saeed, R.A.; Khalek, S.A. Joint power control and user grouping for uplink power domain non-orthogonal multiple access. *Int. J. Distrib. Sens. Netw.* **2021**, 17. [CrossRef]